Impact of Above Cloud Aerosol on the Angular Distribution Pattern of Cloud Bidirectional Reflectance and Implication for Above Cloud Aerosol Direct Radiative Effect

Roy Prouty, Zhibo Zhang, Hongbin Yu, Kerry Meyer

1. Introduction and Theory

With passive remote sensing: the difficulties in calculating the direct radiative effect of above cloud aerosols (DRE_{ACA}) follow directly from the lack of information of the angular dependencies of the radiance fields due to above-cloud aerosols (ACA). Where knowledge of angular distribution model (ADMs) for an unpolluted cloud (CC) scene allow for reasonable estimation of scene irradiance from a single scene reflectance:

$$F_{CC}^{\uparrow,TOA}(\lambda)=P_{CC}(\lambda)\cdot S_0(\lambda)\mu_0 \rightarrow F_{CC,\lambda}^{\uparrow,TOA}=\frac{\gamma_{CC,\lambda}(\mu_0,\phi_0,\mu_v,\phi_v)}{A_{CC,\lambda}(\mu_0,\phi_0,\mu_v,\phi_v)}\cdot S_0(\lambda)\mu_0,$$

(where γ_λ is the spectral BRDF and A_λ is the spectral Anisotropy factor) no analogous representation for the upwelling flux from a polluted (ACA+CC) scene exists.

An investigation of the differences between the CC and ACA+CC ADMs may be able to provide the necessary angular information that will allow for constrained approximations to DRE_{ACA} from sparse observations of the upwelling radiance field of an ACA+CC scene.

In lieu of such information, algorithms for spectral calculation of DRE_{ACA} have been developed that approximate the ADM due to an ACA+CC scene as simply the ADM due to a CC scene. i.e.:

$$DRE_{\lambda,ACA}^{TOA}=\left[\frac{\gamma_{\lambda,CC}}{A_{\lambda,CC}}-\frac{\gamma_{\lambda,ACA+CC}}{A_{\lambda,CC}}\right]S_0(\lambda)\mu_0$$

The preliminary results of an investigation of the differences between this approximation and a 'true' spectral DRE_{ACA} algorithm will be shown here, with emphasis on the angular regions where the two methods agree. Such agreement will be seen to be an indicator of good agreement between the CC and ACA+CC ADMs, otherwise regions where incurred error becomes negligible when integrated spectrally.

2. Methods

i. Calculation of Bulk Scattering Properties (BSP) at bands selected for good representation of solar spectrum
ii. Compute spectral BRDF & A for CC scene
iii. Compute spectral BRDF & A for ACA+CC scene
iv. Calculate spectral DRE_{ACA} (True & Approximate)
v. Spectral integral over the solar spectrum yields DRE_{ACA}

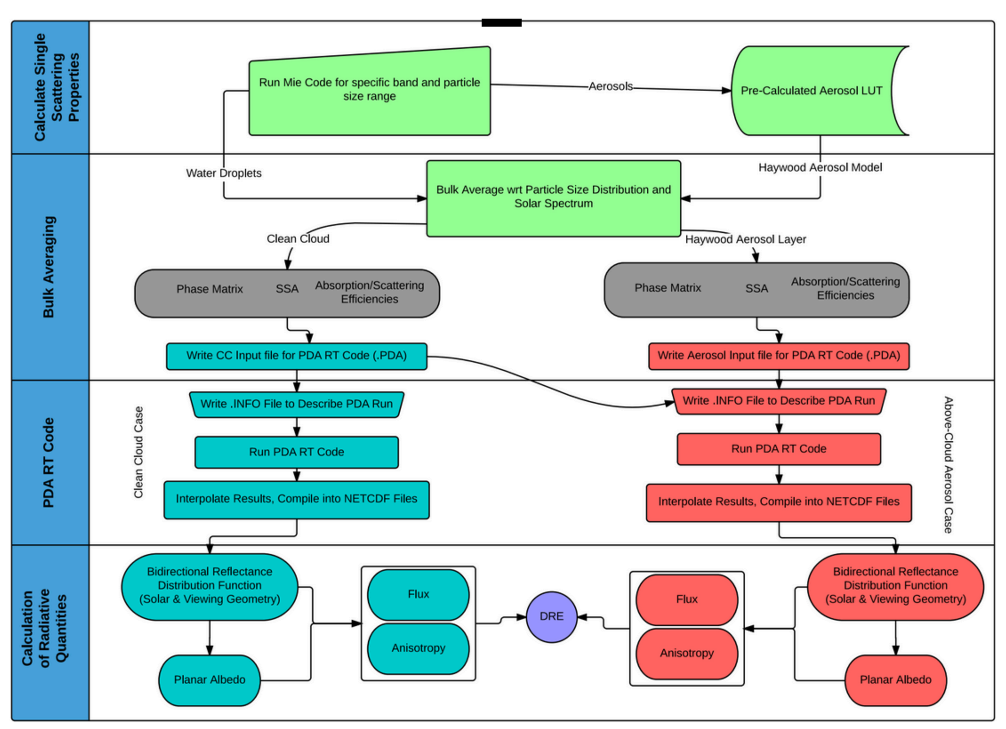

Above: General flow of 1-D PDA RT Code Run from calculation of BSP to the computation of the radiative quantities necessary for analysis.

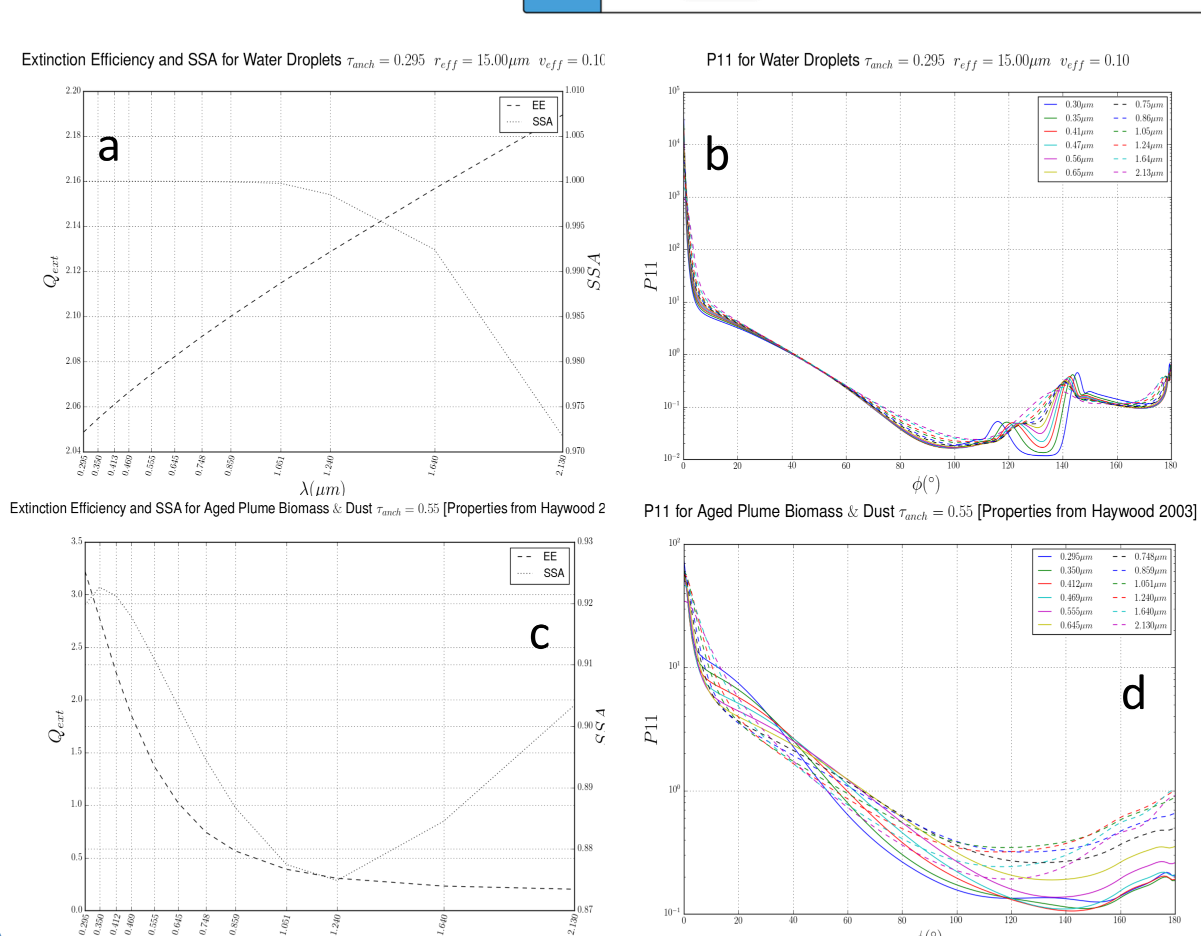

Left: Sample BSP derived from Haywood 2003: Aged Plume. 3-mode PSD (Bio, Bio, Dust). Calculations carried out on band centers chosen to fill solar spectrum adequately.

Extinction Efficiency and single-scattering albedo are given in a & c. The first entry of the phase scattering matrix is given in b & d.

3. Comparison of True and Approximated Algorithms

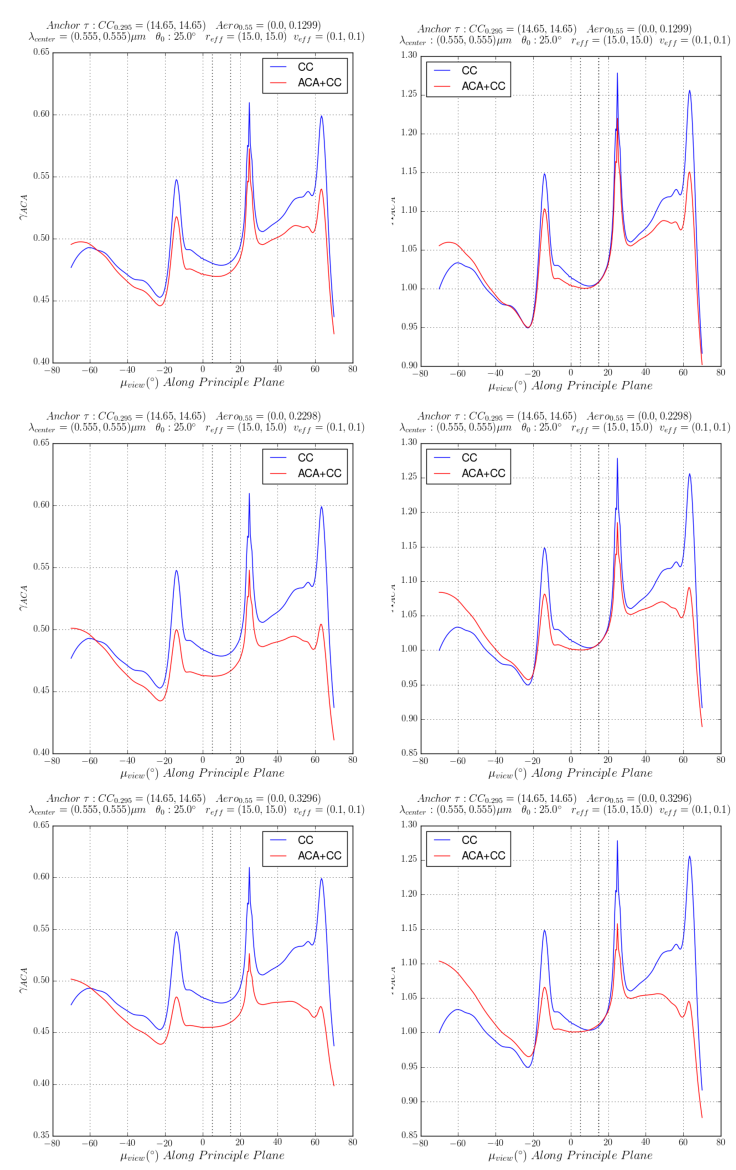

Above: Comparison plots of BRDF (left col) and Anisotropy (right col) along the principle plane. Dashed lines represent azimuthal observation angles at which DRE_{ACA} is later calculated (see far right plots). Blue lines are unpolluted (CC) quantities, and the red are the polluted (ACA+CC) quantities. Three aerosol optical depths (AODs) are shown here, at varying solar zenith angles (SZA): 15, 20, 25 degrees. Relevant information is housed in the parenthesis as follows: (CC, ACA+CC)

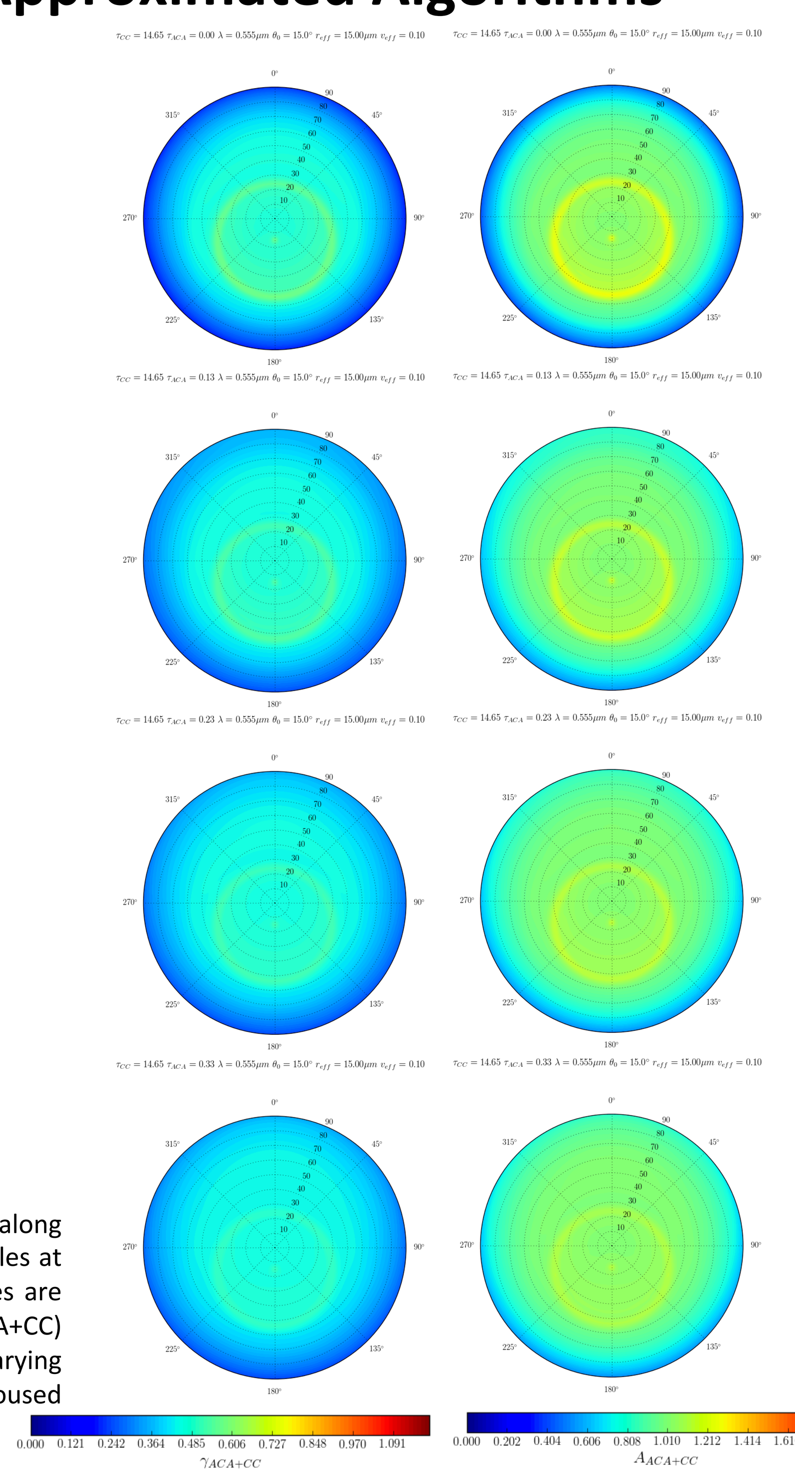

Left: Polar plots of the BRDF (left col.) and Anisotropy (right col.) through increasing AOD (at anchor: 0.00, 0.13, 0.23, 0.33).

In absence of a good baseline, note the relative values and their dependence on AOD. These influence the spectral error as shown above and in the results section.

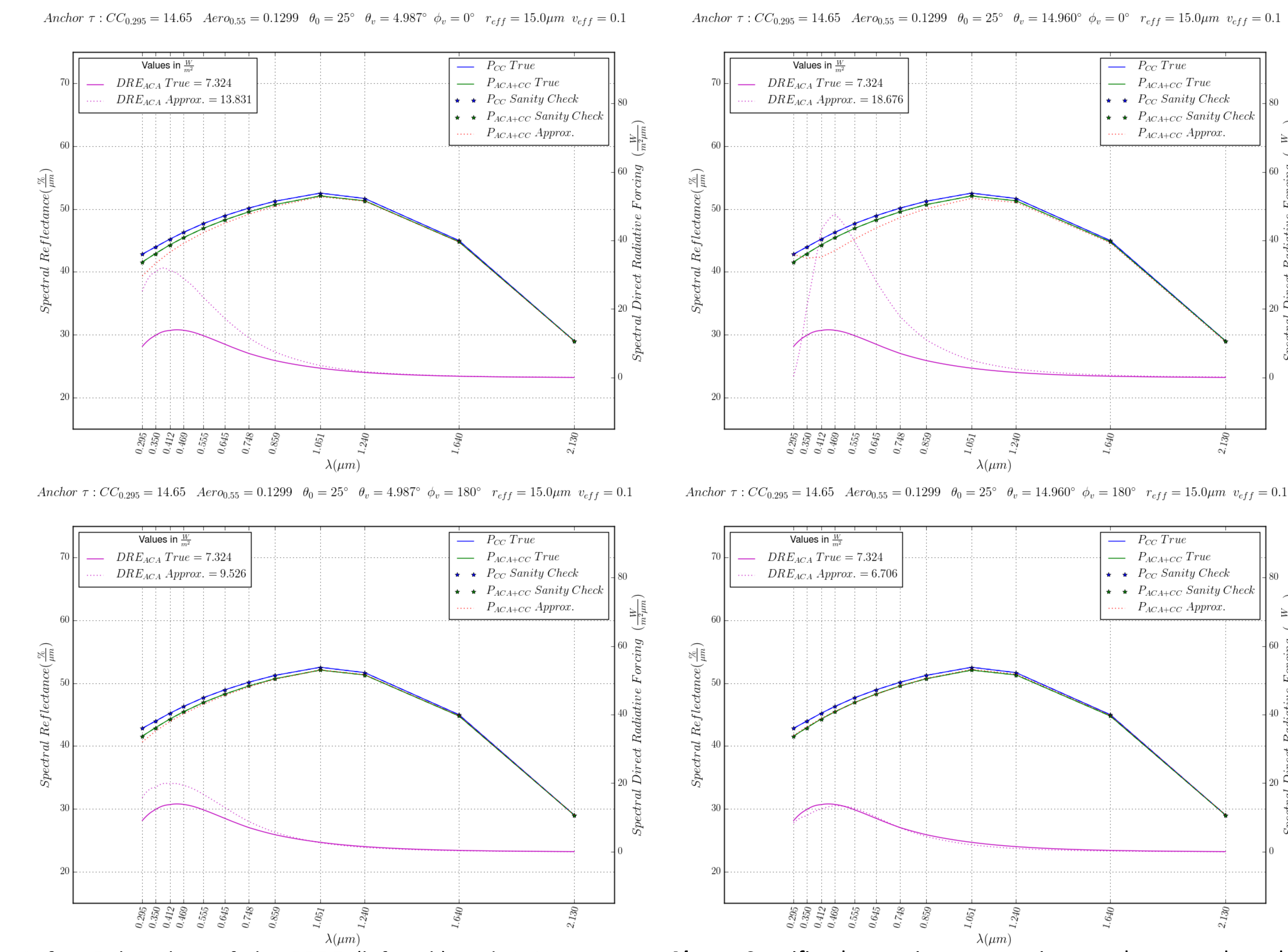

Above: Specific observation geometries are chosen and used to calculate the spectral DRE_{ACA} via the 'true' method (green & solid magenta); via the approximate method (dotted red & magenta lines). The blue line is the unpolluted, spectral planar albedo. The stars represent an alternative calculation scheme used to double-check values.

4. Results

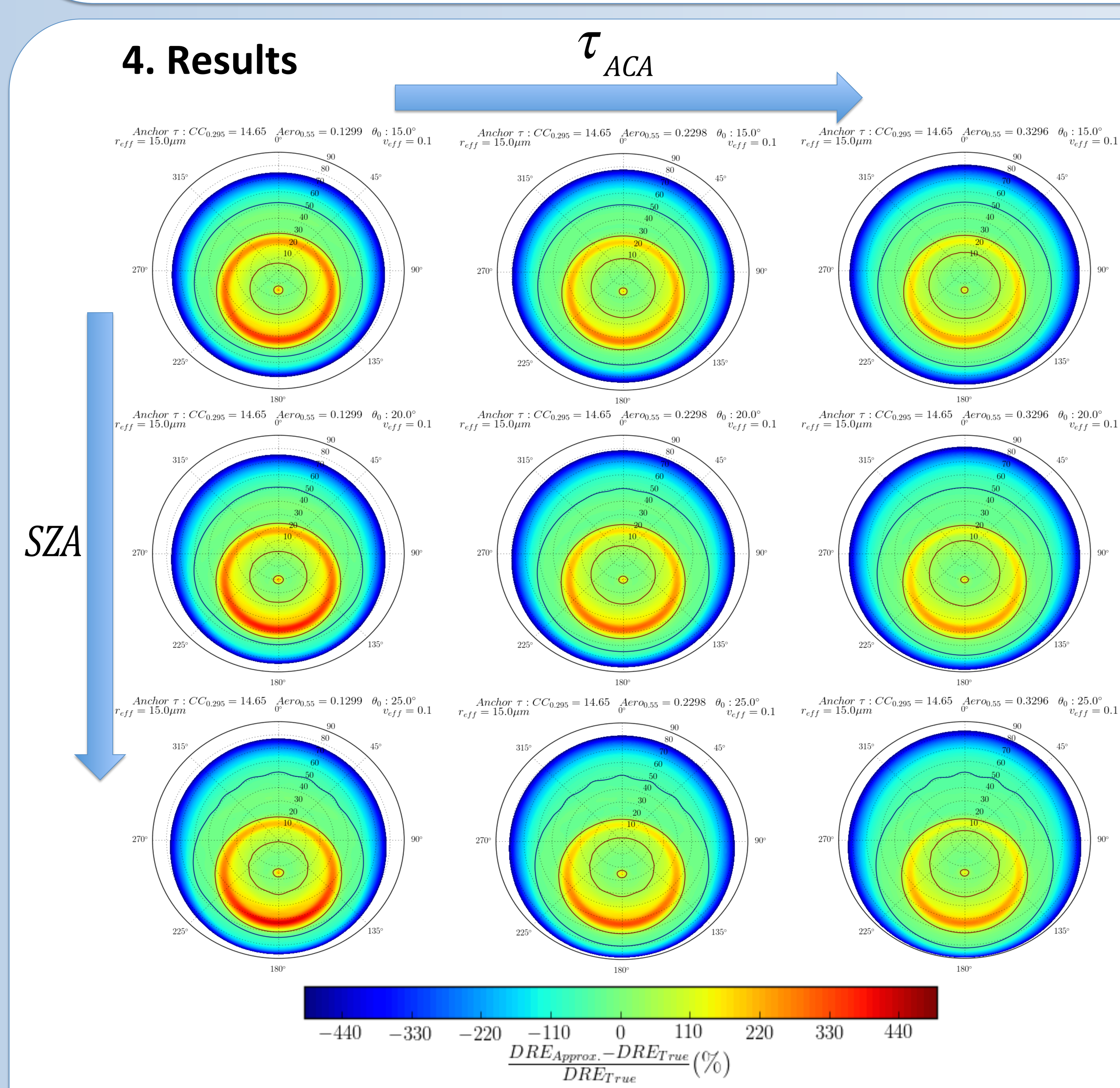

Total (relative) error in DRE_{ACA} incurred by utilizing the approximation to the ACA+CC ADM. The AOD changes across the row while the SZA changes down the column. Potentially significant for passive remote sensing purposes are the outlined regions corresponding to the ±50% error regimes. Angular regions requiring a viewing zenith angle of more than 70 degrees are ignored here and shown as white.

5. Outlook

Handled here is a study of the angular sensitivity of the error incurred via the approximation of ACA+CC ADMs as CC ADMs. For a more complete picture; an investigation of the sensitivity to assumed aerosol model must be completed.

Additionally, these results are from a 1-D PDA RT Code run on specific scenes with specific atmospheric pressure profiles. At smaller (visible) wavelengths, Rayleigh reflectances from pressure-thick layers will influence these results.

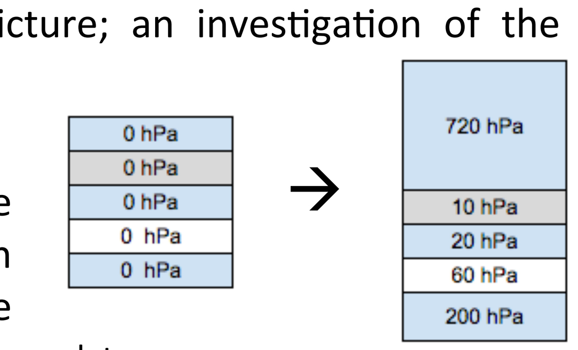

Above-Left: Pressure profiles used for these data
Above-Right: Sample pressure profile for future work (blue: Rayleigh Atmosphere, gray: aerosol, white: cloud)

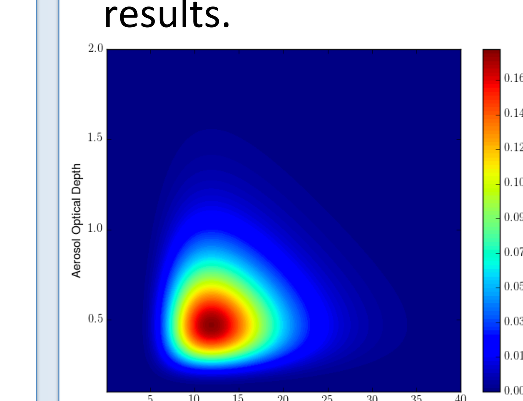

Left: Sample joint probability distribution function for AOD and COD

Also, the regional effects of the aforementioned ADM approximations may be interesting. In which case, realistic spatial distributions of cloud and aerosol optical depth will be developed, the DRE_{ACA} calculated for each permutation, and then the entire ensemble weighted by the distribution.

$$DRE_{ACA,region}=\int_{\rho_{CC}}\int_{\rho_{ACA}} DRE_{ACA}(\tau_{CC},\tau_{ACA})\cdot\rho(\tau_{CC})\rho(\tau_{ACA})d\tau_{CC}d\tau_{ACA}$$

Acknowledgements

The hardware used in the computational studies is part of the UMBC High Performance Computing Facility (HPCF). The facility is supported by the U.S. National Science Foundation through the MRI program (grant nos. CNS-0821258 and CNS-1228778) and the SCREMS program (grant no. DMS-0821311), with additional substantial support from the University of Maryland, Baltimore County (UMBC).

Aerosol Models derived from Haywood, J. M. (2003). The mean physical and optical properties of regional haze dominated by biomass burning aerosol measured from the C-130 aircraft during SAFARI 2000. *Journal of Geophysical Research*, *108*(D13), 8473. http://doi.org/10.1029/2002JD002226